LAUTECH Journal of Engineering and Technology 20 (1) 2026: 209-218

10.36108/laujet/6202.02.0181

Synthesis of Mordenite from Borno White Clay and Assessment of its Water Softening Capacity

[1]Isah, U. A. [1]Mohammed, H. I. and [1,2]Ma'aji, A. M

[1]Department of Chemical Engineering, University of Maiduguri, P.M.B 1069, Maiduguri, Nigeria.
[2]Centre for Entrepreneur, Borno State University, P.M.B 1122, Maiduguri, Nigeria.

Article Info

Article history:

Received: Dec 30, 2025
Revised: Jan 29, 2026
Accepted: Apr 29, 2026

Keywords:

Borno white clay,
Ion exchange capacity,
Mordernite,
Water softening,
Zeolite

Corresponding Author:
uaisah@unimaid.edu.ng

ABSTRACT

This research investigates the local synthesis of mordenite from Borno white clay (BWC), aiming to create a sustainable, low-cost zeolite. The novelty of this work lies in using naturally occurring BWC—previously underutilized for zeolite production in this region—as an aluminosilicate precursor. The study's objectives include collecting, beneficiating, and characterizing BWC to assess its suitability as a zeolite precursor; synthesizing zeolite through hydrothermal crystallization; and evaluating its ion-exchange capacity for water-softening applications. BWC was initially sourced from deposits in Borno State and then calcined at 700°C to transform it into an oxide form. A concentrated sodium hydroxide solution served as the alkaline medium for hydrothermal synthesis at 150°C for 8 hours. Analytical techniques such as X-ray diffraction (XRD), energy-dispersive X-ray fluorescence (EDXRF), Brunauer–Emmett–Teller (BET) surface area analysis, density functional theory (DFT), and ion-exchange capacity (IEC) measurements were used. The results showed that the BWC mainly consists of Quartz, Muscovite, and Orthoclase. Zeolite was successfully synthesized from BWC through hydrothermal methods. XRD confirmed the crystalline formation of mordenite. EDX analysis revealed high contents of sodium, silicon (58.66%), and aluminum (14.67%), which are vital for ion-exchange functions. The BET surface area reached 509.9 m²/g, and pore analysis indicated properties suitable for adsorption and ion exchange, with a beneficial hierarchical micro-mesopore structure. Ion Exchange Capacity (IEC) testing demonstrated the effective removal of calcium ions from hard water, confirming the product's potential for water softening.

INTRODUCTION

The Nigeria Extractive Industries Transparency Initiative (NEITI) report for 2022 identified Borno State as one of the least states that exploit its solid mineral resources (Orji, 2023). Research has shown that there are substantial deposits of white clay suspected to be kaolin in Borno State (Jonathan et al., 2023). The composition and crystal phase of the mineral have yet to be determined. The properties and composition of white clay from other deposits, such as Kanakara (Agbendeh *et al.*, 2021) and Alkaleri (Salahudeen and Idris, 2022), have been confirmed to be kaolin and have been explored for various applications (Christian *et al.*, 2018; Salahudeen and Idris, 2022). Scientific and technical data are scarce on Borno white clay, suspected to be kaolin. The properties and potential industrial applications of this white clay are not well established. Such white clay could be kaolin, feldspar, or diatomite. This study characterizes the white clay and investigates its potential in the synthesis of technical materials, such as zeolites.

Characterizing new clay minerals involves various analytical techniques to determine their composition, structure, and properties. X-ray diffraction (XRD) is a primary method for

identifying the crystalline structure, while Fourier transform infrared spectroscopy (FTIR) and X-ray fluorescence (XRF) provide information about the chemical composition (Ahmed et al., 2021). Additional techniques like scanning electron microscopy (SEM) and transmission electron microscopy (TEM) help visualize the morphology and microstructures (Romero-Guerrero *et al*., 2018).

Previous studies have shown that effective beneficiation is essential for removing organic impurities from clay deposits before characterization (Salahudeen and Idris, 2022). Calcining kaolin is crucial because it activates the material by transforming elements into oxide form, which has an amorphous structure favourable for zeolite formation. Research by Khaled *et al.* (2023) highlighted that calcination temperatures around 600–800°C are ideal for producing oxides of elements in clay, as these conditions promote dehydroxylation without causing excessive crystallization (Mohiuddin *et al.*, 2016).

In Borno State, Nigeria, white clay is mainly found in areas like Biu, Hawul, Shani, Kwaya Kusar, and Bayo. These locations have significant deposits of white clay that could be valuable for industrial uses such as ceramics, paper, paint, zeolites, and medicine because of their fine texture, purity, and chemical stability (Baba et al., 2020). It is essential to thoroughly characterize and explore its potential for industrial applications (Adams *et al.*, 2017).

The main raw materials for zeolite synthesis include silica and alumina. They are readily obtained from natural clays (Agbendeh *et al.*, 2021), aluminosilicate gels (Pyagay *et al*., 2024), diatomaceous earth (Yunusa et al., 2020), feldspar (Amin *et al*., 2023), bentonite (Ma *et al*., 2010), fly ash (Rayalu et al., 2005), rice husk ash (Tawatwachoom and Rungrojchaipon, 2015), waste glass (Majdinasab et al., 2018), and sodium silicate (Isa *et al*., 2018).

Zeolites, a class of crystalline aluminosilicates, are widely recognized for their unique properties, including high ion-exchange capacity, molecular sieving, and catalytic activity. Due to these characteristics, they find diverse applications across industries, from catalysis and environmental remediation to water treatment and detergent formulation. Among various types of zeolites, mordernite is crystalline zeolite characterized by a high silica-alumina ratio and is particularly valued in the detergent industry for its effective calcium ion-exchange properties. These properties enable it to soften water by replacing calcium ions with sodium ions. This ion-exchange capacity is essential for improving detergent efficiency, especially in hard water conditions, by reducing the formation of insoluble salts that can diminish cleaning effectiveness (Koohsaryan *et al*., 2020).

Using zeolite for water softening involves leveraging its unique properties, such as ion-exchange capacity, high surface area, and ability to encapsulate and release active components. Key points to consider when using zeolite for water softening are its ion exchange capacity (Ahmed *et al*., 2018). Zeolite has a three-dimensional framework of silicon and aluminum oxides, forming channels and cavities that can trap water molecules and other ions. It can effectively soften water by exchanging calcium and magnesium ions for sodium ions, which enhances detergent effectiveness. In detergent formulation, its applications include water softening, stain removal, and controlled release. Post-synthesis modifications can improve its properties, such as increasing ion-exchange capacity or enhancing encapsulation efficiency (Rafiani *et al*., 2024). The zeolite can then be blended with other detergent components,

such as surfactants, enzymes, and builders, to create a balanced formulation.

The performance of zeolite in water softening applications depends on its Ion-exchange capacity (IEC). IEC indicates zeolite's ability to swap cations with the surrounding medium. It is usually measured in milliequivalents per gram (meq/g) (Moirou *et al*., 2019). The higher the IEC, the more effective the zeolite is in softening water and improving detergent efficiency. Zeolite's structure contains sodium ions, which can be exchanged for divalent ions like calcium (Ca^{2+}) and magnesium (Mg^{2+}) found in hard water.

IEC can be measured using techniques such as titration or atomic absorption spectroscopy to determine the concentration of exchanged ions before and after treatment (Hewavitharana *et al.*, 2011). Formulations can be tested for performance (cleaning efficiency, foam stability) and effectiveness in softening water, helping to establish optimal concentrations of zeolite A (Bhadja *et al.*, 2015; Skipton *et al.*, 2008). It is essential to ensure compatibility with other detergent components to maintain overall formulation stability and performance. This study focuses on characterizing and utilizing white clay sourced from Borno for Zeolite synthesis and its subsequent application in water softening.

MATERIALS AND METHODS

Materials used in this research include white clay obtained from Biu, Borno State, and reagent-grade chemicals such as NaOH and Al_2O_3.

Characterization of Borno White Clay

White clay was collected from a deposit in Biu, Borno State, Nigeria, with careful attention to prevent sample misrepresentation. Fine powder Borno white clay that passes through a 100-micron mesh was calcined to convert it into oxides of the elements. Approximately 50 g of the white clay was placed into a crucible and heated in a muffle furnace at 900°C for 3 hours. After calcination, the furnace was turned off, and the sample was left to cool gradually to room temperature inside the furnace to prevent thermal shock. The calcined sample was then ground into a fine powder and stored in a desiccator to prevent moisture absorption for characterization and hydrothermal reactions. The characterization of the white clay was conducted using X-ray Diffraction (XRD) and X-ray Fluorescence (XRF) to establish the crystal phases present and the oxides of the elements in the sample.

Hydrothermal Synthesis of zeolite from Borno White Clay

The calcined white clay, obtained through calcination, was carefully weighed to achieve a solid-to-liquid ratio that favoured zeolite A formation, with approximately 25 g of white added to 200 mL of 3 M NaOH solution. The mixture was stirred vigorously for 1 hour at room temperature to create a homogeneous suspension, ensuring thorough interaction between the clay and alkaline solution. After stirring, the mixture was transferred into a Teflon-lined autoclave. The autoclave was then sealed tightly and placed in an oven set to 170°C, where it was maintained for 8 hours to promote crystallisation. These temperatures and durations were based on previous studies (Qoniah *et al*., 2020).

After the crystallisation period, the autoclave was carefully removed from the oven and allowed to cool to room temperature before being opened to prevent sudden pressure changes. The solid zeolite A product was then separated from the residual solution by filtration. The filter cake was washed multiple times with deionised water to remove any residual sodium hydroxide and impurities. Finally, the washed zeolite was dried at 110 °C for 3 hours

to eliminate any remaining moisture and stored in an airtight sample bottle for characterisation and ion exchange experiments.

Characterization of the synthesized zeolite

The synthesized zeolite was characterised. The crystal phases were determined using an X-Ray Diffractometer (XRD), while the morphology and elemental composition were revealed using a Scanning Electron Microscope equipped with an Energy Dispersive X-ray Spectrometer (SEM/EDX). Surface area and pore distribution were measured using a nitrogen adsorption-desorption experiment.

Determination of Ion Exchange Capacity

Ion Exchange Capacity (IEC) of the synthesised zeolite, crucial for its use in detergent production, was measured through a batch ion-exchange experiment. About 1 g of the zeolite sample was weighed and dispersed in 100 mL of a 0.1 M calcium chloride ($CaCl_2$) solution, selected to assess the zeolite's ability to exchange sodium ions for calcium ions, an important aspect in water softening for detergents. The mixture was stirred continuously at room temperature for 3 hours to allow the ion-exchange process to reach equilibrium. After stirring, the solution was filtered to remove the zeolite from the $CaCl_2$ solution. The filtrate was then analysed using atomic absorption spectroscopy (AAS) to determine the calcium ion concentration remaining in the solution, providing data on the exchanged calcium amount. This was used to calculate the ion-exchange capacity, expressed in milliequivalents per gram (meq/g) of zeolite.

IEC was calculated using Equation 1, based on the difference in calcium ion concentration before and after the exchange process (in milliequivalents per gram) (Dyer, 2001; Moirou *et al*., 2019):

$$IEC\ (\frac{meq}{g}) = \frac{(C_i - C_f)V}{mxEW}\ x\ 1000 \qquad Eq.1$$

where, C_i = initial ion (Ca^{2+}) concentration in the 0.1 M $CaCl_2$ solution (mg/L or mol/L); C_f = final ion concentration remaining in the solution using AAS; V = volume of the $CaCl_2$ solution used in the experiment (i.e., 100 mL or 0.1 L) and; m = mass of mordernite (i.e., 1 g) and EW = equivalent weight.

The effect of the initial calcium ion concentration was investigated to gain insight into how the concentration of calcium ions in water influences the process. The experiment was repeated for concentrations of 120, 140, 160, 180, and 200 ppm, respectively.

RESULTS AND DISCUSSION

Mineral phases of Borno White Clay

Figure 1 shows the XRD diffractogram of Borno white clay. The XRD pattern displays clear peaks linked to specific minerals, as reported by Somerset et al. (2004). The quantitative analysis provides the percentage composition of the identified phases. Quartz, Muscovite, and Orthoclase are the dominant crystalline phases identified. The highest intensity peak in the XRD pattern appears at less than 30° 2θ, representing the most prevalent crystalline plane in the sample.

This peak indicates the strongest diffraction and typically corresponds to Quartz, as it is the most abundant phase. Zhou et al. (2013) also confirmed the presence of quartz and muscovite in white clays. The precise 2θ position of the highest intensity is usually listed in the peak data (not directly visible in the document), but it generally appears around 26.6° for Quartz. From Figure 1, it is clear that Quartz is the most prevalent mineral due to its highest peak intensity. Muscovite and Orthoclase are also present, but with comparatively lower peak intensities, suggesting lower concentrations. The presence of these minerals confirms that the Borno

White Clay sample contains silicate minerals, which are typical of natural Borno White Clay deposits.

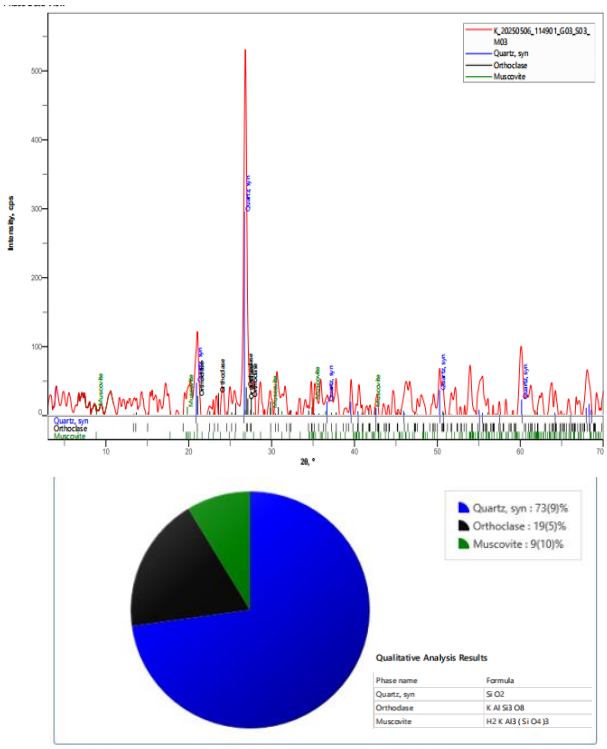

Figure 1: XRD Spectrum of Borno White Clay

X-Ray Fluorescence Composition of Borno White Clay

Silica and alumina compositions are essential requirements for a material to serve as a precursor for zeolite preparation (Agbendeh et al., 2021). Table 1 compares the chemical composition of Borno white clay from XRF analysis with that of kaolin, which was used for zeolite synthesis (Salahudeen and Idris, 2022). The clay has high silica content and low alumina, making it suitable for synthesising various zeolites.

Table 1: X-Ray Fluorescence composition of Borno White Clay

Elemental oxides	**Composition (wt%)**	
	Borno white clay (This study)	**Kaolin** (Salahudeen and Idris, 2022)
SiO_2	70.20	55.0
Al_2O_3	17.30	35.2
Na_2O	-	0.36
K_2O	0.86	1.18
MgO	0.07	0.21
CaO	0.79	0.66
Fe_2O_3	6.43	0.82
TiO_2	2.38	0.08
MnO	0.014	-
P_2O_5	1.53	-

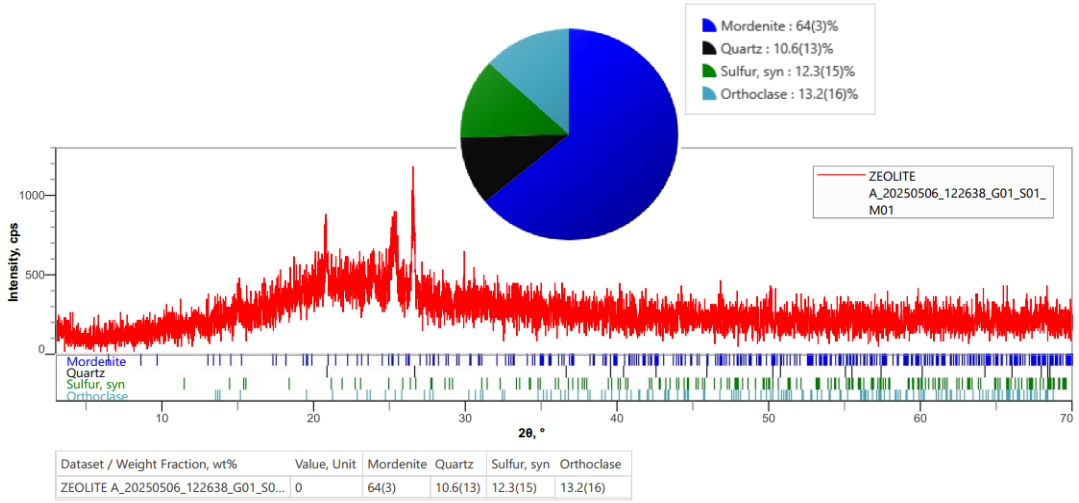

Figure 2: XRD Spectrum of powder synthesized from Borno White Clay

XRD analysis of zeolite derived from Borno White clay

Figure 2 shows the XRD patterns of the powder synthesised from Borno white clay through hydrothermal reaction at a crystallisation time of 8 h. The material exhibits primary peaks at 2θ between 22.2°, 25.7° and 27.7°, which are typical mordernite peaks (Qoniah *et al.,* 2020). Results from Figure 2 depict a mordenite-dominated zeolite. Mordenite is a zeolite used in many applications, ranging from catalysis and water softening to sorbents.

The other peaks are for quartz, sulphur, and orthoclase. ($KAlSi_3O_8$), like zeolites, has a three-dimensional framework of connected tetrahedral sites with a triclinic structure, with Si and Al dispersed in highly ordered tetrahedral coordination, and relatively large voids primarily occupied by sodium (Romero-*Guerrero et al.*, 2018).

Textural characteristics of mordenite derived from Borno White Clay

The textural features of the zeolite were analysed using the Brunauer-Emmett-Teller (BET), Barrett-Joyner-Halenda (BJH), Dubinin-Astakhov (DA), and Dubinin-Radushkevich (DR) methods. The plot of dV(d) (the differential pore volume with respect to pore diameter) against pore volume initially remains constant (i.e., dv(d) = 0 $cm^3/g{\cdot}nm$) because, at smaller pore sizes, the distribution of pores is relatively uniform. Consequently, this results in a steady contribution to the total pore volume. As the pore diameter increases from 1.5 to 3.0 nm, the differential pore volume rises to a peak value of 0.17 $cm^3/g{\cdot}nm$. This indicates a dominant presence of pores of that particular size, where most of the pore volume is concentrated. Beyond this peak (d > 3 nm), the differential pore volume decreases because larger pores become less frequent or contribute less to the total pore volume. Thus, it aligns with the natural distribution, where the number or volume of large pores diminishes.

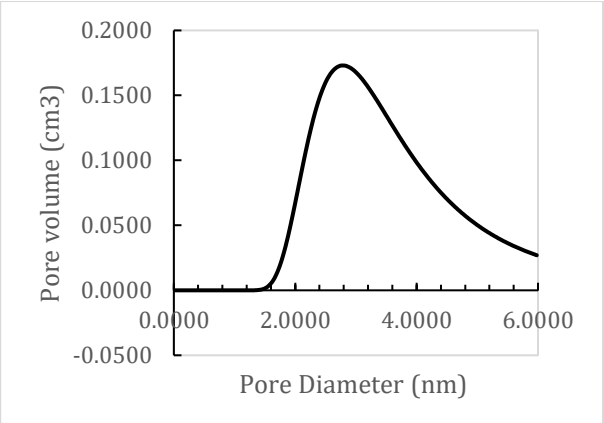

Figure 3: Pore distribution of mordernite, derived from Borno white clay

This pattern reflects typical porous materials, in which small pores are abundant but contribute little, medium-sized pores dominate the volume, and very large pores are scarce. That way, the differential pore volume rises and falls accordingly. Table 2 displays the pore diameter, pore volume, and specific surface area of mordenite. The adsorption energy and the relative affinities of different ions for the zeolite's exchange sites determine the thermodynamics of the ion exchange process (Chudasama *et al.,* 2005). Ions with a higher affinity for the zeolite will displace those with a lower affinity, driving the exchange reaction.

Table 2: Textural Characteristics of Zeolite A Derived from Borno White Clay

Parameters	Modernite
Specific surface area by multi-point BET (m^2/g)	509.9
Total pore volume by BJH method (cm^3/g)	0.3151
BJH mesopore diameter (nm) (minimum)	2.093
DR mesopore diameter (nm) (maximum)	5.634
DA micropore diameter (nm) (average)	2.78
DA adsorption energy (kJ/mol)	0.821
DR adsorption energy (kJ/mol)	4.615

The surface area provides numerous exchange sites, while the pore offers sufficient volume to enable efficient diffusion of ions. Additionally, the energy of adsorption, combined with suitable adsorption energies, facilitates both binding and reversible exchange, significantly influencing their ion exchange capacity (Gackowski, 2020).

The plot of dV(d) versus pore width in Figure 4 appears zig-zag because it shows how the pore volume changes across different pore sizes. Since the material has a mix of pores with varying sizes, each sharp rise or fall corresponds to a significant change in volume for a particular pore width, resulting in the observed shape. The highest peak aligns with the pore width where the largest volume of pores is concentrated, indicating the dominant pore size. The lowest points in Figure 3 show where there are very few or no pores of that size. It is common for microporous or mesoporous materials to exhibit a zig-zag pattern, especially when using the DFT method, because it reveals the detailed pore distribution.

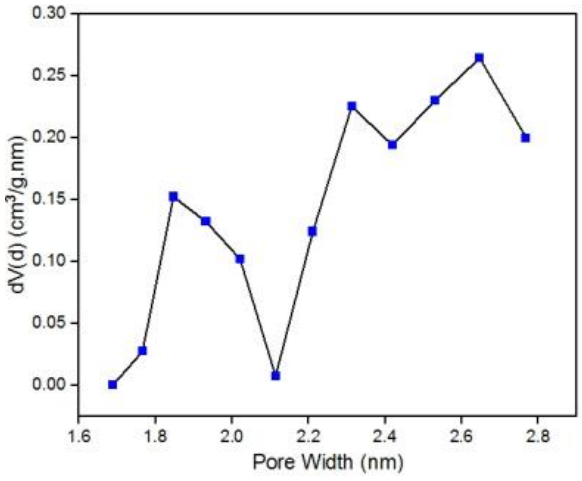

Figure 4: DFT Analysis of a Porous Material

Figure 4 illustrates the Differential Surface Area Distribution (DSAD). DSAD is similar to Figure 3 but instead of volume, it shows the surface area contributed by pores of different widths. The main difference is that Figure 3 focuses on how much space (volume) the pores occupy, whereas Figure 4 emphasises how much surface area those pores provide. When a high value of dS(d) is observed, it indicates that pores of that specific width contribute significantly to the total surface area, which is important for adsorption and catalysis. If the pore width is very small yet has a high dS(d), it suggests the material has a large surface area in tiny pores — a desirable feature for rapid adsorption and reaction rates. Chudasama *et al.* (2005) systematically controlled the pore size of zeolite A through silica deposition and analysed its adsorption properties. Their findings showed that the DSAD increases with pore width, especially in the mesopore range, consistent with the current study.

Ion Exchange Capacity

The IEC of mordernite was calculated from the ion exchange experimental data, ranging from 0.283 to 0.886 meq/g, depending on the initial calcium ion concentration. Figure 5 presents the effect of initial concentration on ion exchange capacity.

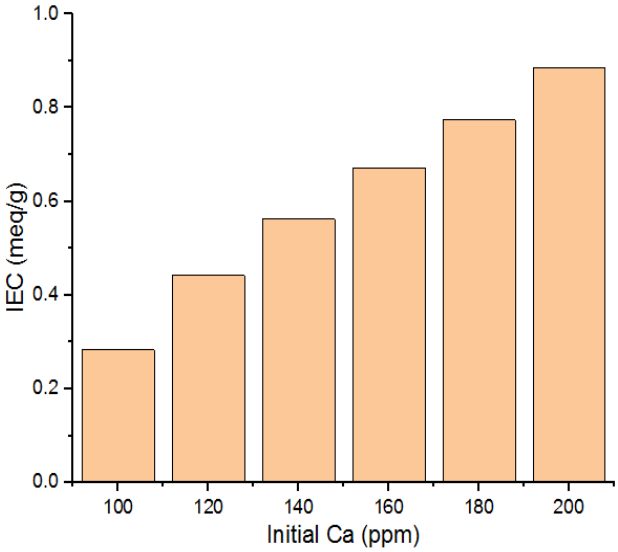

Figure 5: Effect of Initial Concentration on IEC

The exchange process increases with rising Ca ion concentration. This might be due to a large concentration gradient that enhances exchange processes, confirming findings by (Jadhav et al., 2022). Song *et al.* (2015) reported a calcium ion

adsorption capacity of 129.3 mg/g for modified Zeolite A, which equates to approximately 6.45 meq/g. This value is notably higher than the range observed, due to differences in surface area that provide numerous exchange sites, pores with sufficient volume that enable efficient diffusion of ions, and the energy of adsorption coupled with appropriate adsorption energies that allow both binding and reversible exchange, significantly influencing their ion exchange capacity (Gackowski, 2020). These parameters interplay in the IEC of zeolite. However, both results indicate that mordernite has a strong ability to remove calcium ions from solution through ion exchange.

The IEC increases with higher initial calcium concentrations, as shown in Figure 5. The zeolite maintains effective performance even under higher hardness conditions. Its effectiveness across various concentrations supports its practical use in water softening. The measured IEC values demonstrate that mordernite efficiently exchanges Ca^{2+}.

CONCLUSION

After a painstaking analysis leading to very important results for the characterisation of Borno white clay, the synthesis of zeolite from the clay, and the evaluation of its ion exchange capacity, the following conclusions were inferred:

1. Borno White Clay has a silica to alumina ratio of 71% and 17%, respectively, and consists of aluminosilicate minerals such as quartz, orthoclase, and muscovite that are suitable as sources of alumina and silica for zeolite synthesis.
2. Mordenite was synthesised from Borno White Clay using a controlled hydrothermal process. XRD confirmed the formation of mordenite with characteristic peaks, while SEM images revealed the expected cubic morphology. This validates the successful transformation from Borno White Clay to mordenite, a zeolite.
3. The synthesized zeolite exhibited an ion-exchange capacity ranging from 0.283 to 0.886 meq/g. The IEC of the zeolite depends on the initial concentration of calcium. It further indicates strong performance in water softening, making it suitable for detergent applications.

REFERENCES

Adams, F. D., Joseph, M. V, & Shettima, B. (2017). Geochemical investigation of clay minerals in Marte, Borno state, Nigeria. *Arid Zone Journal of Engineering, Technology and Environment (AZOJETE)*, *13*(5), 544–554.

Agbendeh, Z. M., Gimba, C. E., Ande, S., & Ekanem, S. F. (2021). Synthesis and characterization of Zeolite Y from Kankara clay using alkaline fusion method. *Journal of the Chemical Society Nigeria*, *46*(6), 1016–1031. https://doi.org/10.46602/jcsn.v46i6.682

Ahmed, A. N., Sultana, M. S., Zaman, M. N., & Rahman, M. A. (2021). Influence of hard rock dust on the physical and microstructural properties of red ceramic materials. *Journal of the Korean Ceramic Society*, *58*(1), 69–76. https://doi.org/10.1007/s43207-020-00085-2

Ahmed, S., Sanni, K. A., Azeez, O. S., Abdulkareem, A. S., & Oluwafemi, S. (2018). Production of 100 Kg/day of zeolite a as a builder for powdered detergent from Nigerian Ahoko Kaolin using locally fabricated Mini Zeolite Plant. *IOP Conference Series Materials Science and Engineering*, *413*(012064). https://doi.org/10.1088/1757-899X/413/1/012064

Amin, I. I., Wahab, A. W., Mukti, R. R., & Taba, P. (2023). Synthesis and characterization of zeolite type ANA and CAN framework by hydrothermal method of Mesawa natural plagioclase feldspar. *Applied Nanoscience*, *13*, 5389–5398. https://doi.org/10.1007/s13204-022-02756-4

Baba, S., Shettima, B., & Kamale, K. I. (2020). Geological setting and solid mineral potentials of southern Borno, Northeastern Nigeria. *Arid*

Zone Journal of Engineering, Technology and Environment (AZOJETE), *16*(2), 351–362.

Bhadja, V., Makwana, B. S., Maiti, S., Sharma, S., & Chatterjee, U. (2015). Comparative efficacy study of different types of ion exchange membranes for production of ultrapure water via electrodeionization. *Industrial & Engineering Chemistry Research*, *54*(44). https://doi.org/10.1021/acs.iecr.5b03043

Christian, Z. C., John, A., & Shehu, Z. (2018). Chemical investigation of kankara kaolin for its pharmaceutical applications. *Open Access Journal of Translational Medicine & Research*, *2*(1), 11–13. https://doi.org/10.15406/oajtmr.2018.02.00027

Chudasama, C. D., Sebastian, J., & Jasra, R. V. (2005). *Pore-Size Engineering of Zeolite A for the Size / Shape Selective Molecular Separation*. 1780–1786.

Gackowski, M. (2020). *Acid Properties of Hierarchical Zeolites Y*. 25–29.

Hewavitharana, A., Mutucumarana, V., & Kratochvil, B. (2011). An ion exchange atomic absorption method for the determination of ionized calcium at millimolar levels. *Canadian Journal of Chemistry*, *69*(12), 1976–1979. https://doi.org/10.1139/v91-284

Isa, M. A., Chew, T. L., & Yeong, Y. F. (2018). Zeolite NaY synthesis by using sodium silicate and colloidal silica as silica source. *IOP Conference Series: Materials Science and Engineering [ICPEAM 2018]*, *458*, 1–9. https://doi.org/10.1088/1757-899X/458/1/012001

Jadhav, A., Chalak, R., Gholap, V., Ige, V., & Deshmukh, A. (2022). Removal of water hardness by zeolite process. *International Journal of Innovative Research in Technology (IJIRT)*, *9*(1), 1038–1040. https://ijirt.org/master/publishedpaper/IJIRT155506_PAPER.pdf

Jonathan, N., Maina, H. M., & Handawa, P. (2023). Assessment of s olid minerals and s ome elemental oxides in soil of Kwaya Kusar local government area. *Global Scientific Journal*, *11*(5), 89–106.

Khaled, Z., Mohsen, A., Soltan, A., & Kohail, M. (2023). Optimization of kaolin into metakaolin: Calcination conditions, mix design and curing temperature to develop alkali activated binder. *Ain Shams Engineering Journal*, *14*(6), 1–14. https://doi.org/10.1016/j.asej.2023.102142

Koohsaryan, E., Anbia, M., & Maghsoodlu, M. (2020). Application of zeolites as non-phosphate detergent builders: A review. *Journal of Environmental Chemical Engineering*, *8*(5). https://doi.org/10.1016/j.jece.2020.104287

Ma, H., Yao, Q., Fu, Y., Ma, C., & Dong, X. (2010). Synthesis of Zeolite of type A from bentonite by alkali fusion activation using Na2CO3. *Industrial & Engineering Chemistry Research*, *49*(2), 454–458. https://doi.org/10.1021/ie901205y

Majdinasab, A. R., Mann, P. K., Wroczynskyj, Y., Lierop, J. Van, Cicek, N., Tranmer, G. K., & Yuan, Q. (2018). Cost-effective zeolite synthesis from waste glass cullet using energy efficient microwave radiation. *Materials Chemistry and Physics*, *221*(4). https://doi.org/10.1016/j.matchemphys.2018.09.057

Mohiuddin, E., Isa, Y. M., Mdleleni, M. M., Sincadu, N., Key, D., & Tshabalala, T. (2016). Synthesis of ZSM-5 from impure and beneficiated Grahamstown kaolin: Effect of kaolinite content, crystallisation temperatures and time. *Applied Clay Science*, *119*, 213–221. https://doi.org/10.1016/j.clay.2015.10.008

Moirou, A., Vaxevanidou, A., Christidis, G. E., & Paspaliaris, I. (2019). Ion exchange of Zeolite Na-Pc with Pb2+, Zn2+, and Ni2+ ions. *Clays and Clay Minerals*, *48*, 563–571. https://doi.org/10.1346/CCMN.2000.0480509

Orji, O. O. (2023). *Nigeria Extractive Industries Transparency Initiative (NEITI)*.

Pyagay, I. N., Svakhina, Y. A., Titova, M. E., Dronova, V. R., & Miroshnichenko, V. V. (2024). Determination of Zeolite NaA (LTA) synthesis parameters from technogenic silica gel for water softening. *Silicon*. https://doi.org/10.1007/s12633-024-03177-4

Qoniah, I., Prasetyoko, D., Hartati, & Nikmah, Y. L. (2020). Optimization of hydrothermal temperature and time parameters in the synthesis of hierarchical ZSM-5 from kaolin by taguchi method. *Materials Science Forum*, *981 MSF*,

104–111. https://doi.org/10.4028/www.scientific.net/MSF.981.104

Rafiani, A., Aulia, D., & Kadja, G. T. M. (2024). Zeolite-encapsulated catalyst for the biomass conversion: Recent and upcoming advancements. *Case Studies in Chemical and Environmental Engineering*, *9*(100717). https://doi.org/10.1016/j.cscee.2024.100717

Rayalu, S. S., Udhoji, J. S., Meshram, S. U., Naidu, R. R., & Devotta, S. (2005). Estimation of crystallinity in flyash-based zeolite-A using XRD and IR spectroscopy. *Current Science*, *89*(12), 2147–2151.

Romero-Guerrero, L. M., Moreno-Tovar, R., Arenas-Flores, A., Marmolejo Santillán, Y., & Pérez-Moreno, F. (2018). Chemical, mineralogical, and refractory characterization of kaolin in the regions of Huayacocotla-Alumbres, Mexico. *Advances in Materials Science and Engineering*, *2018*. https://doi.org/10.1155/2018/8156812

Salahudeen, N., & Idris, F. (2022). Effects of beneficiation on the characteristics of Alkaleri Kaolin. *Engineering Journal Chiang Mai University*, *29*(1), 12–20.

Skipton, S., Dvorak, B., & Niemeyer, S. (2008). *G08-1491 Drinking water treatment: Water softening (Ion Exchange)*.

Somerset, V. S., Petrik, L. F., White, R. A., Klink, M. J., Key, D., & Iwuoha, E. (2004). The use of X-ray fluorescence (XRF) analysis in predicting the alkaline hydrothermal conversion of fly ash precipitates into zeolites. *Talanta*, *64*(1), 109–114. https://doi.org/10.1016/j.talanta.2003.10.059

Song, J., Liu, M., & Zhang, Y. (2015). Ion-exchange adsorption of calcium ions from water and geothermal water with modified zeolite A. *Separations: Materials, Devices and Processes*, *61*(2), 640–654. https://doi.org/10.1002/aic.14671

Tawatwachoom, T., & Rungrojchaipon, P. (2015). In-situ synthesis of Zeolite A, Zeolite P and Zeolite Y/carbon composite with carbonaceous rice husk ash. *Pure and Applied Chemistry International Conference 2015 (PACCON2015)*, 1–5.

Yunusa, S., Ahmed, A. S., Yusuf, M., Abubakar, M., & Bawa, S. G. (2020). Characterization of synthesized Zeolite Socony Mobile5 (ZSM-5) from Bularafa Diatomite. *Arid Zone Journal of Engineering, Technology and Environment (AZOJETE)*, *16*(4), 717–724.

Zhou, H. M., Qiao, X. C., & Yu, J. G. (2013). Influences of quartz and muscovite on the formation of mullite from kaolinite. *Applied Clay Science*, *80–81*, 176–181. https://doi.org/10.1016/j.clay.2013.04.004.